Plasma Dynamics Laboratory
Technical Report No. 67-3

July , 1967

NON-EQUILIBRIUM PROPERTIES OF MAGNETOPLASMAS

by E.H. Holt, J.H. Noon, and R.L. Gunshor

Semiannual Status Report No. 1

NASA Grant No. NGR 33-018-075

September 1, 1966 - February 28, 1967

Rensselaer Polytechnic Institute
Troy, New York

NON-EQUILIBRIUM PROPERTIES OF MAGNETOPLASMAS

by E. H. Holt, J. H. Noon and R. L. Gunshor

Rensselaer Polytechnic Institute

SUMMARY

Studies are in progress on instabilities in an arc plasma; on the current convective instability of collision dominated plasmas; and on the occurrence of non-Maxwellian electron velocity distributions in plasmas. The arc plasma facility has been constructed and put into operation. With argon gas fed continuously through a hollow cathode and the resultant ionized gas collimated by a magnetic field in the region between the anode and cathode, the arc has been operated up to a current of 80 amps and Langmuir probe measurements of the electron temperature and density have been made.

The characteristics of the current convective instability in the hollow plasma column typical of some plasma accelerators have been investigated. Langmuir probe measurements of the radial form of the perturbed electron density reveal that the rotating helix is concentrated in the outer region of the plasma. The instability occurs at a lower value of the critical magnetic field for a hollow plasma than for a regular positive column of the same diameter. For both the regular and the hollow positive column the use of measured plasma density profiles in the numerical evaluation of the stability criterion is shown to give improved agreement between theory and experiment. The theory of the current convective instability has been generalized to include the case of an applied magnetic field with shear. The new theory predicts that when the total helical magnetic field and the helical density perturbation have the same sense, the plasma is destabilized and a mode switch should occur at a certain value of the azimuthal component of the magnetic field. In the opposite case the plasma is predicted to be stabilized and the $m = 1$ mode is predicted to be dominant. An experiment has been performed and these predictions have been confirmed.

A comprehensive study of the occurrence of non-Maxwellian electron velocity distributions in an active nitrogen plasma has been made. It is shown that such distributions occur below a critical current level in the discharge and within a certain critical time after the initiation of the discharge.

INTRODUCTION

Non-equilibrium properties vitally affect the performance of such plasma devices as thrustors for space flight and MHD generators. The main objective of the present program is the measurement and analysis of non-equilibrium conditions in such plasmas, including instability phenomena and the presence of non-Maxwellian velocity distributions. An important secondary objective is the development of methods of increasing the stability of the plasmas being studied.

This is the first status report to be issued on this grant.

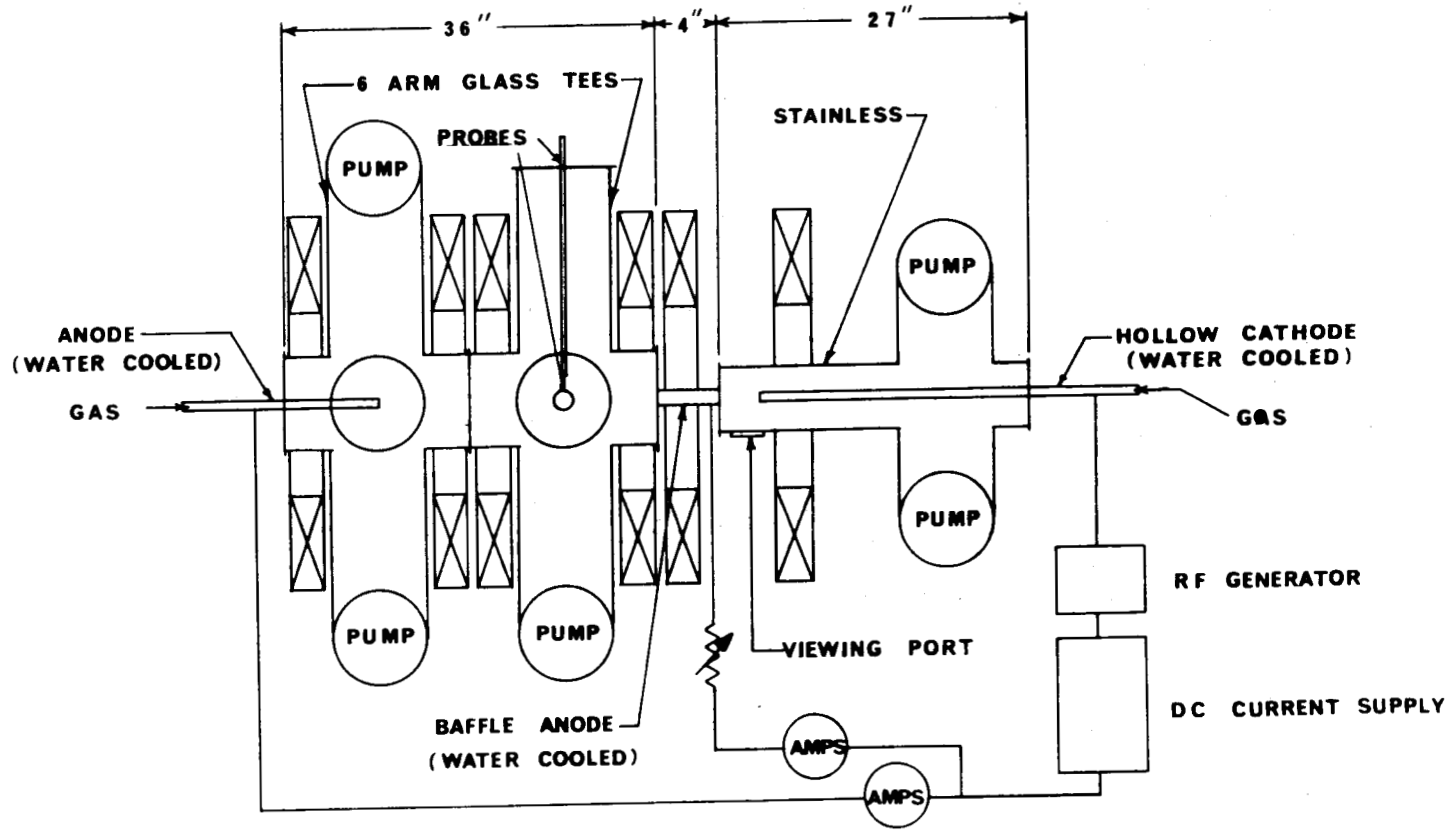

Figure 1

Schematic of the hollow cathode, gas fed arc plasma facility.

HIGH ENERGY DENSITY PLASMA FACILITY

A hollow cathode, gas fed arc plasma machine has been constructed for the study of instabilities and instability-related transport phenomena in a high energy density, highly ionized plasma. This type of gas discharge has been described in the literature and is found to exhibit properties which makes it attractive for these studies. The machine bears important similarities to devices which are under active development for space propulsion.

In particular it has been found that it becomes relatively quiescent under certain operating conditions and recent results indicate r.m.s. fluctuation levels lower than those achieved on Q machines while at the same time the plasma is orders of magnitude more energetic.

The hollow cathode, gas fed arc is composed basically of a hollow tube at cathode potential, through which a continuous gas flow is maintained, and an anode, through which a gas may also flow. The plasma is formed inside and near the end of the cathode tube by processes still not fullv understood. The plasma fills the space between the electrodes whilst the neutral particles are pumped away. From previous experiments, we expect electron densities up to about 10^{14}/c.c. and electron temperatures from 2 to 20 eV along with nearly complete ionization. During operation of the arc, the cathode, made of refractory material (sometimes impregnated with thorium or barium) operates at thermionic emission temperatures. These arcs have been operated with several gases, sometimes with a second gas fed into the anode, and ionized by the plasma originating from the cathode.

The Rensselaer hollow cathode arc has been constructed so as to maximize both the versatility of electrode position and electrical configuration, and to permit access to a wide range of diagnostic probes. A schematic drawing of the system is shown in Fig. 1. The main section of the cell is constructed using two, 6 inch i.d., 6-arm glass crosses. The tantalum cathode, initially made of 1/8 inch diameter tubing, is located within a stainless steel cell having a glass viewing port. Some difficulty was experienced with stray rf breakdown (an rf voltage is used together with the dc applied voltage to start the arc). This trouble was eliminated by using a boron nitride shield together with a glass tube as shown in Fig. 2.

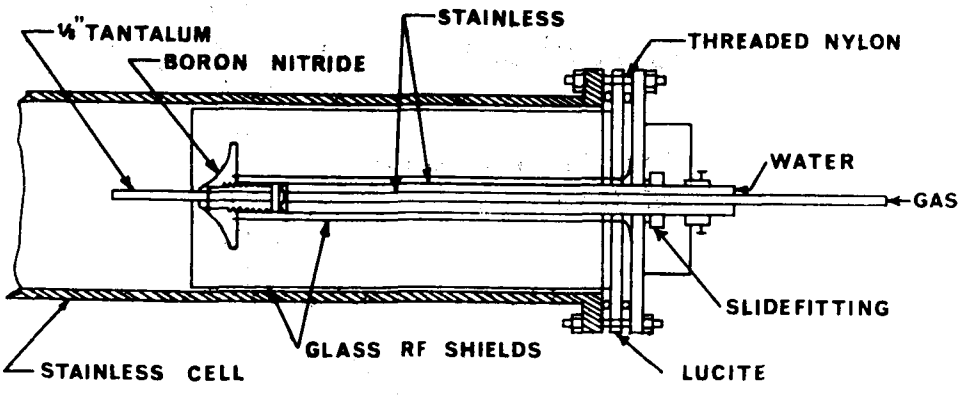

Figure 2

Detailed design drawing of the hollow cathode assembly

The high ionization level is maintained by pumping neutrals away while the active plasma is magnetically confined. This requires a relatively high pumping speed to handle the gas flowing into the hollow cathode: from four to six 4 inch diffusion pumps are used to achieve the necessary pumping speed.

Continuous operation of the arc has been in general restricted to low current conditions, of the order of 20 amps, although the arc is started at about 70 amps. These levels are considerably below the limits of the device; arc currents of 100 to 200 amps should be within design limits. Some initial operating data are shown in Table 1. In order to obtain operation at lower cathode temperatures, bariated tungsten cathodes are being tested as a possible replacement for tantalum.

Table 1

Operating Characteristics of the Hollow Cathode, Gas Fed Arc Plasma

Argon flow Atmos-cc/sec	Arc Volts	Arc Amps	B_o (gauss)
0.27	37.2	22.0	1300
	41.0	50.0	1300
0.39	37.0	22.7	1300
	39.0	50.0	1300

The initial diagnostics are aimed at determining the basic plasma parameters such as electron and ion density and temperature. Thus far the measurements have been of electron temperature and ion density by means of Langmuir probes. One of the problems confronting these measurements is the high energy density in the central "core" of the arc. This necessitates the rapid sweep of the probe through the plasma and requires circuitry for the interpretation of such measurements. A probe circuit has been constructed to provide for these measurements, and some initial data has been obtained. Figure 3 shows a probe characteristic for the probe outside the energetic central region; the probe has not yet been passed through the central part of the arc. The measured values of density and temperature are in the range previously reported in similar devices.

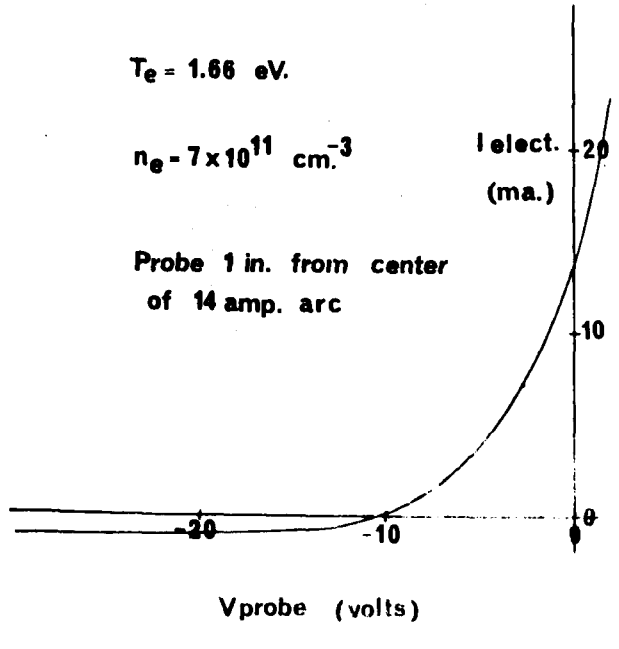

Figure 3

Typical Langmuir probe characteristic in the outer region of the arc.

THE CURRENT CONVECTIVE INSTABILITY IN COLLISION DOMINATED PLASMA COLUMNS

Introduction

Work under previous NASA grant (NsG 48) established the importance of small transverse components of the magnetic field upon the onset of the current convective or helical instability of the positive column. This work has been extended by measurements of the radial density profile of the plasma which permit more accurate comparison between theory and experiment; by studies of the hollow positive column which is the plasma configuration used in the linear Hall accelerator: and by an experimental and theoretical analysis of the effect of an azimuthal magnetic field component on the stability of the hollow positive column.

Radial Profile of the Perturbation Density for the Helical Instability in a Positive Column

In their analysis of the helical instability of the positive column, Kadomtsev and Nedospasov (ref. 1) assumed that the perturbed density varied radially as a first order Bessel function

$$n_1(r) \propto J_1(\beta_1 r)$$

where $n_1(0) = n_1(R_B) = 0$, and R_B is the outer radius of the cell. This assumption was later confirmed by the more complete mathematical treatment of Johnson and Jerde (ref. 2). Holter and Johnson (ref. 3) calculated the radial profile for the time-averaged density by assuming that there was a rotating helix superimposed on the steady state density of the positive column. They showed that the zero-order Bessel function form for the unperturbed density showed a shift into that of a first order Bessel function as the amplitude of the helix grew.

Recently Itoh et al (ref. 4) reported measurements of the time averaged density profile in an effort to confirm Holter and Johnson's results. Their results showed qualitative agreement in that the profile shifted slightly but no conclusion as to the functional form of the perturbed density was possible. Previous measurements reported by Artsimovich and Nedospasov (ref. 5) did not show agreement with Holter and Johnson due to the fact that their measurements were made in a turbulent regime where many higher order modes were present.

We have been able to confirm the theoretically predicted form of the density perturbation in the regular positive column by measuring the perturbed ion density with only the m = 1 helical mode present. To avoid the non-linear effects of the fully developed instability, the m = 1 mode is excited at magnetic field strengths slightly below the critical value by employing the procedure described by Huchital and Holt (ref. 6).

For these measurements a discharge cell of 6.5 cm outer radius and 2 meter length was used. The magnetic field was uniform to 1% over a length of

40 cm. Four probes, spaced 90° apart were located at two cross sections. These were used both to indicate onset of the instability and to assure that only the m = 1 mode was present. A bellows-mounted, radially moveable probe, 0.13 mm in diameter and 6 mm long, was used for the density measurements. The density was determined by measuring the ion saturation current to the probe. The perturbed density profile was determined by measuring the amplitude of the oscillations in the probe current at the frequency of the instability. This was done with a Hewlett-Packard - 310A wave analyzer. All measurements were made in a helium discharge.

Typical density profiles for the positive column are shown in Fig. 4.

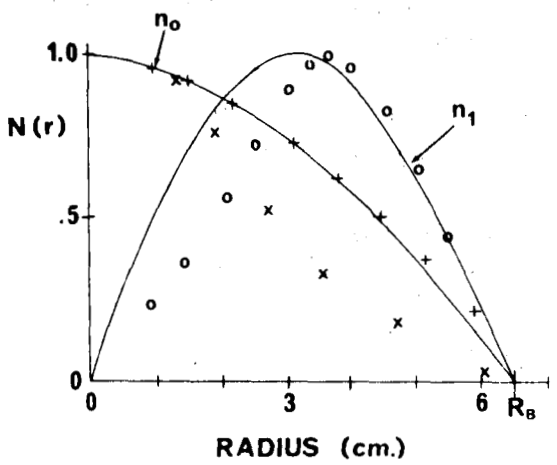

Figure 4

Density profiles for positive column. Solid lines are theoretical curves for zero-order, n_o, and perturbed, n_1, densities. Crosses (+) are measured values of n_o at B = 0g. (x) are measured values of n_o at onset of instability (B = 435 g). Circles (o) are measured values of perturbed density, n_1. 100 ma helium discharge at pressure of 0.16 torr.

The solid lines represent the theoretical curves for the steady state and perturbed density profiles. The steady state profiles were taken both at zero magnetic field and at a value of magnetic field slightly below critical to demonstrate the constriction of the column caused by the electrodes being outside the magnetic field region (ref. 7). As can be seen, the measured profile for the perturbed density is reasonably approximated by the first order Bessel function assumed by Kadomtsev and Nedospasov.

Critical Magnetic Field Measurement for the Helical Instability in a Hollow Plasma Column

We have examined the effect of a longitudinal magnetic field on the stability of a helium plasma in the shape of a hollow cylinder. This study is particularly relevant to the configurations used in several plasma accelerator designs. The hollow positive-column cell was 2 meters long and the inner and outer radii were 0.95 and 6.5 cm respectively. Four probes spaced 90° apart were located at two outer cross-sectional locations separated by 40 cm along the axis of the cell. At two other cross-sections evenly spaced between these were sets of two probes 180° apart and a radially movable probe was located midway between the outer sets of probes. Onset of an instability was detected both by monitoring the noise voltage to a probe and by the sharp change in the longitudinal electric field E_z at the critical magnetic field B_c. Azimuthal and longitudinal phase shift measurements were employed, as in earlier work (ref. 8), to identify the

m = 1 helical mode present. The solenoidal magnetic field used was uniform to within one percent over the region of the plasma between the probes. However, since both electrodes were outside the solenoid, a constriction of the plasma column occurs in the uniform magnetic field region above a field of around 300 gauss. The effect of this constriction on the zero order radial electron density profile at low pressures on the stability of the plasma has been shown by Adati et al (ref. 7). At higher pressures this constriction is less noticeable, but a pressure of 0.18 torr was selected to avoid striations in the discharge and to avoid the co-existence of quiescent and turbulent regions in the plasma column.

To derive numerical values from the stability criterion (refs. 1, 2, 9), it is necessary to evaluate integrals which depend on the radial form and the gradient of the zero order electron density $n_o(r)$ and the perturbed density $n_1(r)$. The radial density for the hollow cell may be written, Belousova (ref. 9)

$$n_o(r) = J_o(\beta r) + B\, Y_o(\beta r)$$

with boundary conditions $n(R_A) = 0 = n(R_B)$, where J_o and Y_o are the zero and second order Bessel functions respectively, B is a numerical constant, R_A and R_B are the inner and outer radii of the vessel respectively, and $\beta = (Z/D_a)^{1/2}$, where Z = the rate of ionization in the column and D_a = the ambipolar diffusion coefficient. For our experimental arrangement B = 2.22 and $\beta = 3.54/R_B$.

The measured profile for $n_o(r)$ for zero magnetic field, shown graphically in Fig. 5(a), agrees with the theoretical form. However the measured density profile for a longitudinal field just below the critical value B_c, also shown in Fig. 5(a), shows evidence of constriction of the type reported by Adati et al (ref. 7) and it is this profile which we have used as representing the appropriate form of the unperturbed radial density.

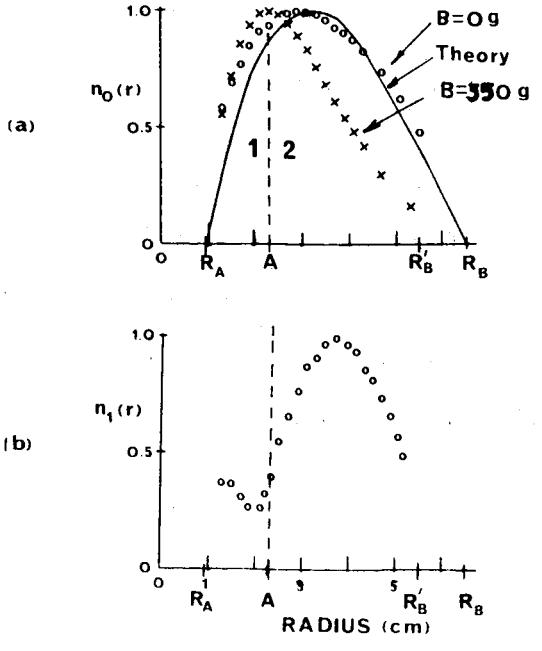

Figure 5

(a) The measured zero-order radial electron density in the hollow positive column for zero magnetic field, the theoretical density for this case, and the measured electron density profile for a longitudinal magnetic field just below the critical value B_c, showing constriction of the plasma.

(b) The measured radial form of the perturbed electron density $n_1(r)$.

For the radial form of the perturbed density $n_1(r)$ Belousova (ref. 9) chose a mathematically tractable form

$$n_1(r) = J_1(\beta r) + C\, Y_1(\beta r)$$

with boundary conditions $n_1(R_A) = 0 = n_1(R_B)$.
However, as indicated in Fig. 5(a), the actual form of the perturbation will be determined by the different electric fields which arise in regions 1 and 2 on either side of A, the position of peak electron density where $dn_o/dr = 0$. Fig. 5(b) shows measured profiles of $n_1(r)$ obtained from the AC component of the probe signal in the ion saturation region. The perturbation is clearly concentrated in the region between A and R_B and, because of the constrictions of the plasma column, falls short of the outer radius at some value R_B'. The profile of the perturbation therefore departs markedly from the form assumed by Belousova (ref. 9).

Numerical evaluation of the stability criterion is simplified by using an analytical form for the radial electron density, so we have approximated the zero order density by

$$n_o(r) \propto J_o\left[\frac{2.405}{(R_B' - A)}(r - A)\right] .$$

evaluated between the limits $A < r < R_B'$, and the perturbed plasma density by the function

$$n_1(r) \propto J_1\left[\frac{3.83}{(R_B' - A)}(r - A)\right]$$

evaluated between the same limits.

Fig. 6 shows the results of theoretical calculations both for the hollow

Figure 6

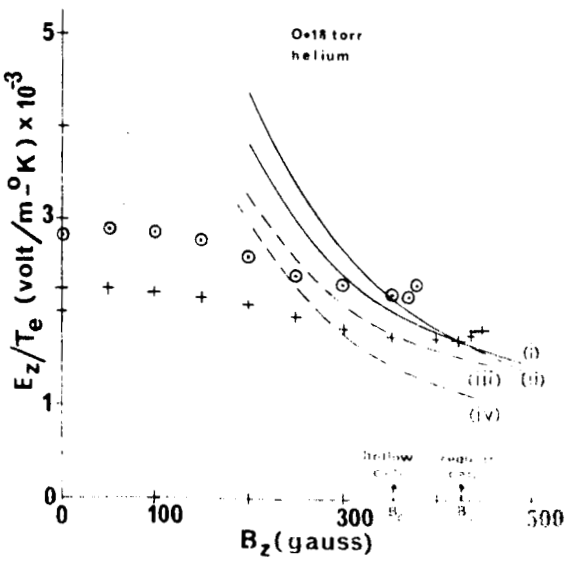

Theoretical curves of longitudinal electric field over electron temperature, E_Z/T_e, versus longitudinal magnetic field B_Z. Curves (i) and (ii) represent the hollow and regular columns, using the measured profiles for $n_1(r)$ and $n_o(r)$. Curves (iii) and (iv) represent the hollow and regular columns using the analytic expressions for $n_1(r)$ and $n_o(r)$ after Belousova (ref. 9) and Kadomtsev and Nedospasov (ref. 1). The experimental points for hollow and regular column cells are indicated by circles and crosses respectively.

cell and a regular positive column of the same outer radius. In the classical regime, lower values of E_z with increasing B_z correspond to reduced plasma diffusion and thus serve as a measure of the confining effect of the longitudinal magnetic field. The region below the curve of E_z/T_e versus B_z should represent the limits of stable conditions for the experimental configuration. A locus of experimental points is obtained by measuring E_z with increasing B_z and should reveal the onset of the instability with an abrupt change in slope on crossing the theoretical curve (ref. 10) at $B = B_c$.

As shown in Fig. 6 the theoretical calculations based on the analytical forms of the radial electron density used by Kadomtsev and Nedospasov and by Belousova, predict increased stability for the hollow column over the regular column, whereas our calculations based on the measured profiles indicate almost identical stability criteria. However the increased electron loss at the inner wall of the hollow cell results in a higher value of E_z for the hollow cell than the regular cell. Consequently the experimental loci of measured values of E_z/T_e cross the theoretical curves at a lower magnetic field B_z for the hollow cell than the regular cell, which means that experimentally the critical field B_c for onset of an instability is lower for the hollow cell. Fig. 6 shows the improved agreement in predicting the actual critical magnetic field, both for the hollow and the regular positive column cell, obtained by correctly modelling the radial form for $n_0(r)$ and $n_1(r)$. This study emphasizes the importance of understanding the physical processes appropriate to the experimental conditions when predicting stability criteria.

The Current Convective Instability in a Magnetic Field with Shear

The equations describing the behavior of a weakly ionized, collision dominated plasma in a longitudinal magnetic field have been generalized to include the effect of an azimuthal component of the magnetic field and the stability criterion for the onset of the helical instability in a magnetic field with shear has been developed. In the experiment the azimuthal magnetic field component was generated by passing a current-carrying conductor through the center of a hollow, cylindrical plasma cell. The theory predicts that when the total helical magnetic field and the helical density perturbation have the same sense, the plasma is destabilized and the critical value of the strong, longitudinal magnetic field is reduced. For this same case a mode switch from the $m = 1$ mode to the $m = 2$ mode is predicted at a certain value of the azimuthal magnetic field. In the opposite case, the plasma is predicted to be stabilized against the helical instability and no mode switch from the $m = 1$ mode is predicted. These predictions are confirmed by the experiment.

The stabilizing effect is similar to that reported by Chen and Mosher (ref. 12) for a thermally ionized, resistive plasma subjected to a magnetic field with shear. The present work shows that shear stabilization also applies to weakly ionized, collision dominated plasmas if the configuration of the shear field is properly related to the geometry of the helical instability. Von Gierke and Wohler (ref. 13) reported the first experimental evidence of the effect of an azimuthal magnetic field component on the onset

of this instability.

A magnetic field of the form $\bar{B} = (0, B_\phi, B_z)$ was included in the equation of motion of the plasma electrons. This was then combined with the usual equation of motion for the ions and the continuity equation to obtain two equations for the density and potential of the plasma in a manner similar to that used by Kadomtsev and Nedospasov (ref. 1). The stability criterion against the growth of a plasma perturbation of the usual helical form, $\exp\left[i\,(kz + m\phi + \omega t)\right]$, was developed from these equations. It can be written in the following simplified form:

$$(G_1 + H_1)k^4 + (H_2 + H_3 d)k^3 + (G_2 + H_4 + H_5 d)k^2 + (H_6 + H_7 d)k + G_3 + H_8 + H_9 d = G_4 k$$

where $d = B_\phi \tau_e E_z/T_e$, and τ_e is the reciprocal of the electron-neutral collision frequency. For $B_\phi = 0$ and $m = 1$ this reduces to $G_1k^4 + G_2k^2 + G_3 = G_4k$ which is identical to the criterion derived by Kadomtsev and Nedospasov (ref. 1) for the case of a single helix in a longitudinal magnetic field. The coefficients G_1 through G_4 and H_1 through H_9 involve a variety of integrals over the zero order plasma density, n_o, and the perturbed plasma density, n_1, as well as depending upon the magnetic field components.

Thus,

$$G_1 = -\left[1 + (eB_z \tau_e/m)^2\right] I_1 \left[I_2 (I_4 - m^2 I_5) + I_1 \left(\frac{b_e Z}{b_i D_e} I_2 + \frac{I_3}{1+y}\right)\right]$$

where $y = (b_i/b_e)\left[1 + (e\tau_e/m)^2 (B_z^2 + B_\phi^2)\right]$, b_e, b_i are the electron and ion mobilities respectively, Z is the ionization rate and D_e is the electron diffusion coefficient. I_1 through I_5 are integrals involving the radial dependence of the plasma density.

For example,

$$I_1 = \int_{R_1}^{R_2} r\, n_o\, n_1^2\, dr \quad \text{and} \quad I_4 = \int_{R_1}^{R_2} n_1 \frac{d}{dr}\left(r\, n_o \frac{dn_1}{dr}\right) dr$$

Complete expressions for all the coefficients are given by Reynolds (ref. 14) and will be given in a technical report.

The stability criterion has been numerically evaluated and the results are shown in Fig. 7. Although the calculations were made for the particular plasma column which was studied experimentally, the qualitative effect of an applied azimuthal component of the magnetic field is more generally applicable. This effect is that a negative azimuthal magnetic field component stabilizes the column. This corresponds to the sense of the total, helical magnetic field being opposed to that of the helical density perturbation.

We wish to emphasize the importance of using appropriate limits of integration when evaluating the integrals which occur in the stability

criterion. These limits should define that part of the plasma which is characterized by a negative gradient of the zero order plasma density for increasing radius, because that is the part of the plasma which supports the growth of the helical perturbation (ref. 15). The choice is simply $R_1 = 0$ and $R_2 = R_B$ (the outer radius) in the case of the regular positive column. However, in the case of a hollow column the limits should be taken between the value of r at which $dn_o/dr = 0$ which we will designate as A and the outer radius. Thus $R_1 = A$ and $R_2 = R_B$. These limits have already been discussed in the preceeding section.

When a shear field is applied the value of the lower limit, A, becomes a function of B_ϕ. In order to evaluate this dependence and also to determine the complete radial form of n_o it is necessary to generalize the equation which describes the radial dependence of n_o to the case of the positive column immersed in a magnetic field with shear. The following equation has been obtained:

$$\frac{d^2 n_o}{dr^2} + \frac{1}{r}\frac{d n_o}{dr} + \frac{e^2}{mk} B_\phi \frac{E_z}{T_e} \frac{d n_o}{dr} + n_o \left(\frac{Z}{D'_a} + \frac{e^2 \tau_e}{mkr} B_\phi \frac{E_z}{T_e} \right) = 0$$

where D'_a is the ambipolar diffusion coefficient in a longitudinal magnetic field (B_z). Analog computer solutions of this equation for positive and negative values of B_ϕ in the case where the column is hollow are shown in Fig. 8(a). Experimental data taken with a radially movable probe are shown for comparison in Fig. 8(b). We see that the point A moves significantly in response to a change in B_ϕ and this effect was taken into account in the calculations.

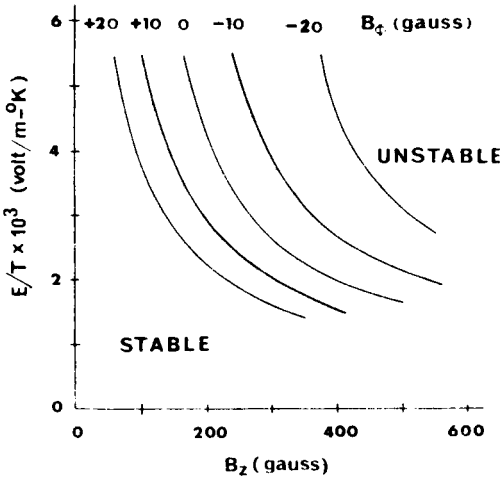

Figure 7

Theoretical predictions calculated from the stability criterion for the hollow column (outer radius 6.5 cm, inner radius 0.95 cm) which was studied experimentally. Helium gas, pressure = 0.18 torr. B_ϕ is taken to be positive when the current generating the azimuthal field (B_ϕ) is parallel to the discharge current.

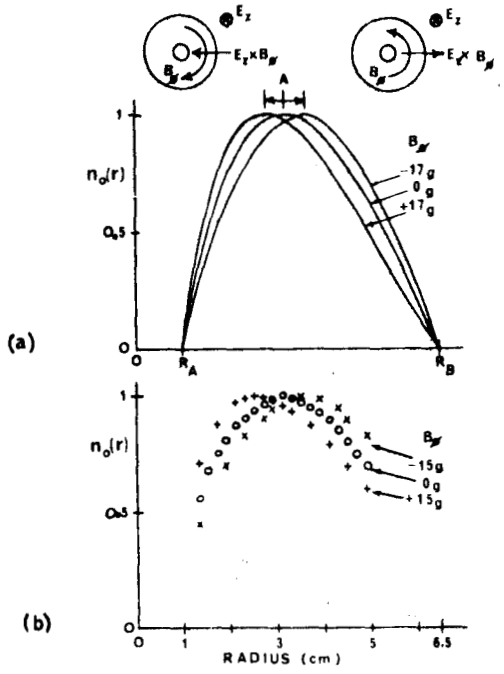

Figure 8

Radial plasma density profiles in the same hollow column showing effect on the $E_z \times B_\phi$ drift. The theoretical curves (a) are analog computer solutions of Eq. (2). Experimental results with a radially moveable probe are shown in (b).

Consideration of the overall change in the radial form n_o as a function of B_ϕ predicted by this equation permits a qualitative interpretation of the effect of B_ϕ on stability to be made. Figure 8 shows that an increase in B_ϕ is accompanied by a reduction in the average value of dn_o/dr in the region of the plasma where the helical density perturbation grows. This means that the value of the radial electric field, E_r, caused by the ambipolar diffusion of the plasma, will be reduced. Since E_r acts to stabilize the column (ref. 15) the plasma will be destabilized in this case, as predicted by the theory.

For the experimental study the hollow discharge cell described in the preceeding section was used, through which three water-cooled conductors were passed. Current (typically 100-200 amp.) flowing through these conductors generated the azimuthal field. All the experiments were done in helium.

Typical experimental results for the critical longitudinal magnetic field, B_c, and the frequency of oscillation at onset, f, as a function of the azimuthal component of the magnetic field, B_ϕ, are compared with theoretical curves in Fig. 9. Quantitative agreement, which requires knowing the electron temperature and the exact form of the density profiles under experimental conditions is within the limits of experimental uncertainty.

OCCURRENCE OF NON-MAXWELLIAN VELOCITY DISTRIBUTIONS IN NITROGEN PLASMAS

Preliminary measurements of non-Maxwellian electron velocity distributions in nitrogen afterglow plasmas performed under a previous NASA grant (NsG 48) have been followed up in the present period by a comprehensive study of the active nitrogen plasma. A new experimental cell and associated microwave circuitry permits the measurement of noise radiation, microwave

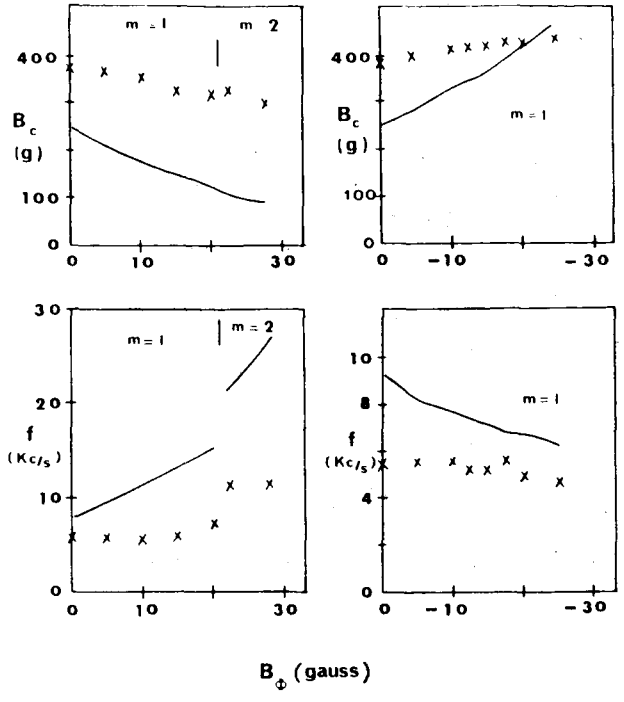

Figure 9

Comparison of theory (solid lines) with experiment for the characteristics of the helical instability in the same hollow column. B_c is the critical value of the longitudinal magnetic field and f is the frequency of oscillation of the instability at onset. Helium pressure = 0.18 torr. Mode switching in the destabilizing case is shown.

absorption and reflectivity. It is shown that non-Maxwellian electron velocity distributions occur below a certain critical current level in the discharge and within a certain critical time after the initiation of the discharge.

A gated microwave radiometer was used to monitor changes in the noise emission spectrum of the plasma electrons as the magnetic field in which the plasma was immersed was swept through a small range on either side of that value where the electron cyclotron frequency was equal to the microwave radiometer frequency. This technique was originally employed by Fields, Bekefi and Brown (ref. 16) to determine the steady state form of the electron velocity distribution in the positive column of a number of gases (excluding nitrogen).

A simple expression for the distribution function in terms of two parameters p and y is

$$f(v) \propto \exp\left(- p\, v^{y}\right)$$

where the parameter p is related to the mean electron energy $\langle u \rangle$ in terms of non-integer gamma functions by

$$p = \frac{m}{2 \langle u \rangle} \left[\frac{\Gamma(5/y)}{\Gamma(3/y)} \right]^{y/2}$$

If the exponent y = 2, the distribution is Maxwellian, and $y < 2$ or $y > 2$ correspond respectively to distributions rich in or deficient in high energy electrons compared to the Maxwellian distribution of the same mean energy.

For nitrogen the electron-neutral collision frequency $\nu(v)$ is an increasing function of v over almost all electron energies (ref. 17) of

interest. When the radiation temperature T_r is calculated by the method of Fields it is found to peak at $\omega_B = \omega$ for $y > 2$, remain constant for $y = 2$, and show a dip at $\omega_B = \omega$ for $y < 2$.

A separate effect which must be considered is the gradual decrease in electron temperature in the positive column with increasing longitudinal magnetic field B (ref. 18) which occurs even when there is a Maxwellian electron velocity distribution. This is associated with reduced diffusion of electrons to the vessel walls with increasing B and is also reflected in a lower ionization rate and a reduced longitudinal electric field in the plasma. An example of this effect in the case of nitrogen is shown in Fig. 10. Experimentally measured changes in radiation temperature which occur with increasing magnetic field for a steady-state nitrogen plasma are shown to agree with calculated values based on the theory of von Engel and Steenbeck (ref. 18) for a plasma with a Maxwellian electron velocity distribution. As B is increased by 100% (from 2,000 to 4,000 gauss) T_r decreases by approximately 25% (from 17,000 to 13,000°K), corresponding to a change in longitudinal electric field of approximately 25%. There is a monotonic decrease in radiation temperature with increasing magnetic field but no resonant behavior of T_r occurs as the magnetic field is swept through the value of 3,250 gauss where $\omega_B = \omega$.

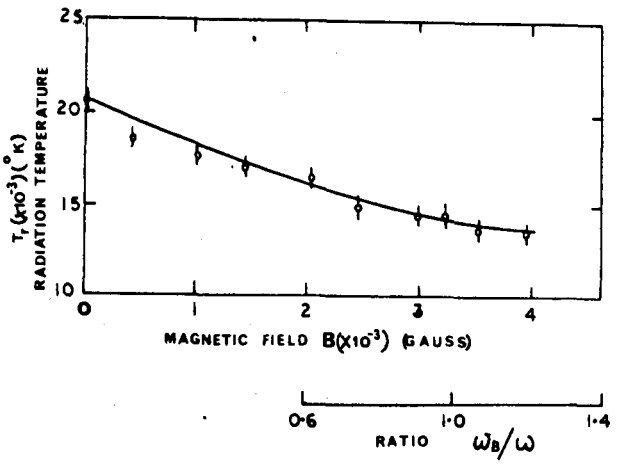

Figure 10

Change in radiation temperature of a steady state nitrogen discharge at 0.7 torr as the magnetic field is increased from 0 to 4,000 gauss. The experimental points are compared with a theoretical curve derived from von Engel and Steenbeck (ref. 18) (vertical lines represent uncertainty in measured values).

The plasma studied consisted of a positive column discharge established in a 4 mm diameter pyrex tube inserted through the broad face of a section of X band waveguide and making an angle of approximately 10° with the waveguide axis. The effective length of the plasma-filled waveguide section was 7.6 cm. The magnetic field was uniform to within 1% over the length of the plasma.

A repetitive discharge was initiated at 100 cycle/second rate using a hard tube pulser. The energy input could be varied from less than a tenth of a millijoule to several millijoules, by changing the current in the discharge or the duration of the voltage pulse. This was too low an energy to give rise to any significant heating of the neutral gas molecules. By means of a variable delay the two microsecond wide gate pulse for the radiometer could be adjusted in time until it corresponded to the time in the active discharge at which data was to be taken.

The radiation temperature at any instant could be measured by measuring the microwave noise power emitted from the plasma and performing a separate experiment to determine the absorptivity and reflectivity of the plasma. A block diagram of the microwave circuit is shown in Fig. 11. T_r was monitored as a function of time in the absence of an applied magnetic field and again at a fixed time while sweeping the magnetic field through a 40% range on either side of 3,250 gauss. All measurements in nitrogen were carried out at a pressure of 0.7 torr.

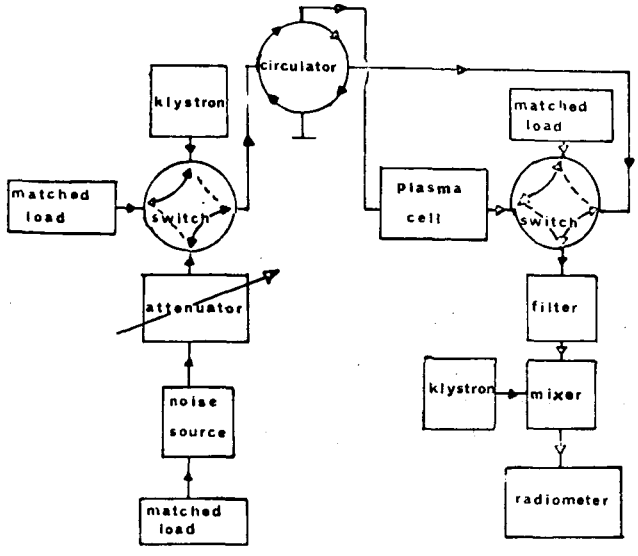

Figure 11

Block diagram of the microwave circuit. By adjusting the waveguide switches it is possible to measure either (i) noise power transmitted by the standard source through the plasma, (ii) the absorption coefficient of the plasma, or (iii) the reflection coefficient of the plasma.

The plasma density was derived by two independent methods. From the measured current density and the appropriate value of the electron drift velocity based on the value of the reduced electric field E/p, the plasma density was estimated to be 1.4×10^{11} cm^{-3} for the highest current discharge used. This value agrees with calculations based on the measured microwave absorption of the effective length of the plasma column in the waveguide. The reflection coefficient of the plasma under these conditions was 0.1.

As a control for the nitrogen measurements, the radiation temperature was monitored for the active discharge in argon gas under the same conditions of sweeping the magnetic field. The results, shown in Fig. 12, are similar to those obtained by other workers at S band frequencies (ref. 16). The pronounced peak in the radiation temperature at electron cyclotron resonance indicates that the electron velocity distribution is deficient in high energy electrons as compared with a Maxwellian of the same average energy. This agreement in results serves as added confirmation of the validity of extending the experimental technique to X band frequencies.

In distinction from the argon results it was found possible to obtain a Maxwellian electron velocity distribution in the active nitrogen discharge provided that both the discharge current and the duration of the voltage pulse were sufficiently large. This result is shown in the upper part of

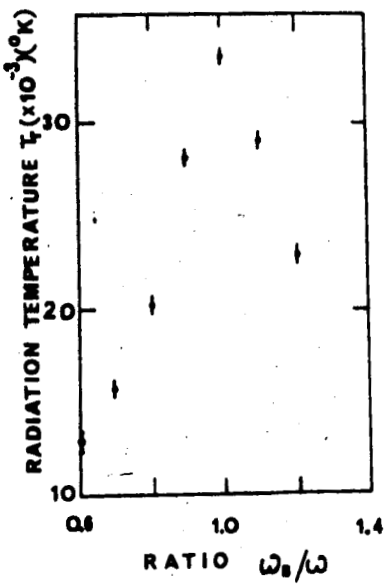

Figure 12

Experimental measurements of T_r for an argon discharge under the same conditions of sweeping the magnetic field as for nitrogen in Fig. 13.

Fig. 13 where for a discharge current of 360 mA and a pulse width of 50 μsec there is the expected monotonic decrease in T_r with increasing B with no resonance behavior at the magnetic field value where $\omega_B = \omega$. However for lower currents and for shorter pulse widths T_r shows pronounced peaking around the value of B for which $\omega_B = \omega$, indicating departure from a Maxwellian velocity distribution.

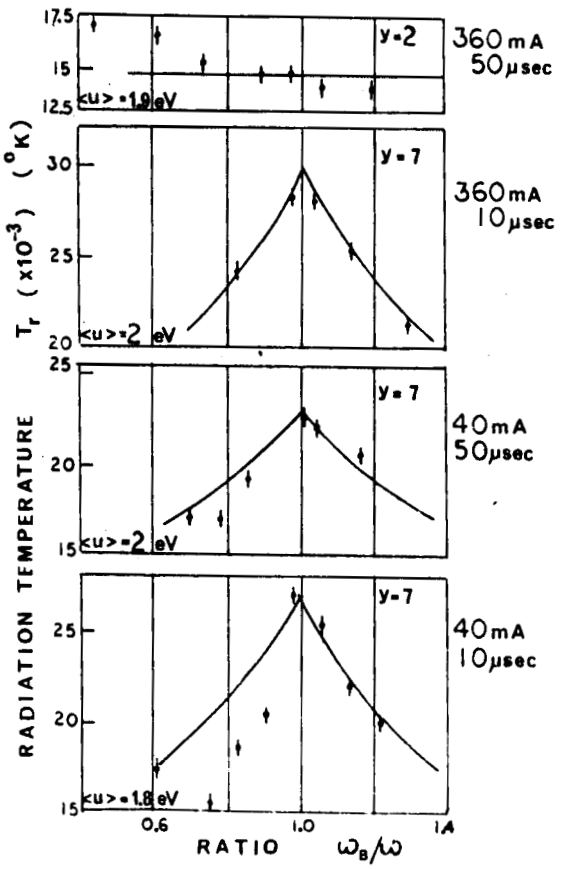

Figure 13

Experimental measurement of the radiation temperature in the active discharge for a range of discharge parameters in nitrogen at 0.7 torr. The magnetic field is swept from 2,000 to 4,000 guass around the value of 3,250 gauss where $\omega_B = \omega$.

It is clear that below certain current levels and within certain times from the initiation of the plasma there is a non-Maxwellian electron velocity distribution. These two parameters are not expected to be entirely independent of each other.

PLANS FOR THE NEXT PERIOD

The characteristics of the arc plasma will be studied using probe techniques. The investigation of the effect of a magnetic field with shear on the current convective instability will be continued. The occurrence of non-Maxwellian electron velocity distributions in nitrogen plasmas will be extended to cover the afterglow regime.

PAPERS PRESENTED

Changes in the Electron Velocity Distribution of a Nitrogen Plasma. J. H. Noon, P. R. Blaszuk and E. H. Holt. 19th Annual Gaseous Electronics Conference, Atlanta, October, 1966. Bull. Amer. Phys. Soc., 12, 217 (1967).

Stabilization of a Positive Column Discharge by Transverse Magnetic Fields. J. F. Reynolds, E. H. Holt and W. C. Jennings. 8th Annual Meeting of the Division of Plasma Physics of the Americal Physical Society, Boston, November, 1966. Bull. Amer. Phys. Soc., 12, 804 (1967).

REFERENCES

1. B. B. Kadomtsev and A. V. Nedospasov, "Instability of the Positive Column in a Magnetic Field and the Anomalous Diffusion Effect", J. Nucl. Energy, C1, 230 (1960).

2. R. R. Johnson and D. A. Jerde, "Instability of a Plasma Column in a Longitudinal Magnetic Field", Phys. Fluids, 5, 988 (1962).

3. O. Holter and R. R. Johnson, "Finite Amplitude Instability of a Positive Column", Phys. Fluids, 8, 333 (1965).

4. S. Itoh, M. Kawaguchi and K. Yamamoto, "Radial Density Profile in a Positive Column with a Longitudinal Magnetic Field", Phys. Fluids, 9, 2535 (1966).

5. L. L. Artsimovich and A. V. Nedospasov, "The Radial Distribution of Plasma of a Positive Column in a Magnetic Field", Soviet Phys.-Doklady, 7, 717 (1963).

6. D. A. Huchital and E. H. Holt, "Sub-Threshold Excitation of the Kadomtsev Instability", Appl. Phys. Letters, 8, 321 (1966).

7. K. Adati, Y. Iida, T. Sekiguchi and N. Yamada, "Stabilizing Effect of Radial Plasma Density Distribution on the Helical Instability", Phys. Fluids, 9, 1464 (1966).

8. D. A. Huchital and E. H. Holt, "Modes of the Kadomtsev Instability", Phys. Rev. Letters, 16, 677 (1966).

9. L. E. Belousova, "Hollow Positive Column in a Longitudinal Magnetic Field", Soviet Phys. Tech. Phys., 11, 658 (1966).

10. T_e as a function of B was obtained from the measured values of E_z using the dependence of T_e on E/p for helium given by Hoh (ref. 11).

11. F. C. Hoh, "Low Temperature Plasma Diffusion in a Magnetic Field", Rev. Mod. Phys., 34, 267 (1962).

12. F. F. Chen and D. Mosher, "Shear Stabilization of a Potassium Plasma", Phys. Rev. Letters, 18, 639 (1967).

13. G. von Gierke and K. Wohler, "On the Diffusion in the Positive Column in a Longitudinal Magnetic Field", Nucl. Fusion Suppl., Part 1, p. 47 (1962).

14. J. F. Reynolds, "The Effect of an Azimuthal Magnetic Field on the Helical Instability in a Hollow Positive Column", Ph.D. Thesis, Rensselaer Polytechnic Institute (1967).

15. F. C. Hoh, "Screw Instability of a Plasma Column", Phys. Fluids, 5, 22 (1962).

16. H. Fields, G. Bekefi and S. C. Brown, "Microwave Emission from Non-Maxwellian Plasmas", Phys. Rev., 129, 506 (1963).

17. A. G. Engelhardt, A. V. Phelps and C. G. Risk, "Determination of Momentum Transfer and Inelastic Collision Cross Sections for Electrons in Nitrogen Using Transport Coefficients", Phys. Rev., 135, A1566 (1964).

18. R. J. Bickerton and A. von Engel, "The Positive Column in a Longitudinal Magnetic Field", Proc. Phys. Soc., A69, 468 (1956).